International Journal of Engineering and Advanced Technology (IJEAT)
ISSN: 2249-8958 (Online), Volume-3 Issue-4, April 2014

# A Comparative Study of XFEM and EFGM in Solving Frictional Contact Problems

**Azher Jameel**

***Abstract*— In this paper, the extended finite element method (XFEM) and the element free Galerkin method (EFGM) have been employed to model and simulate the contact type of nonlinearities caused by the discontinuities due the frictional contact. In order to model these discontinuities, few modifications are made in XFEM and EFGM to incorporate these discontinuities in the formulation. The contact interface between the two bodies is modeled by applying an appropriate enrichment function. The classical approximate solution is enriched with the Heaviside jump function to simulate the contact behavior between the two surfaces. Gaussian quadrature has been used for the numerical integration of the weak formulation. Finally, three model problems are solved using XFEM and EFGM and the results obtained by the two techniques are compared with each other. The results obtained by XFEM show a good agreement with the results obtained by EFGM.***

***Key words*—XFEM, EFGM, slip criterion, slip rule, penalty factor, level set, Heaviside jump function.***

## I. INTRODUCTION

There are various problems in everyday life that involve frictional contact between two surfaces like metal forming processes, semi-rigid connections in steel structures and various biomechanics problems like the determination of stresses in human joints and implants. There are a number of methods such as finite difference method [1], finite element method [2], boundary elements method [3], element free Galerkin method [4] and extended finite element method [5] that are available to model and simulate various types of discontinuities in solid mechanics problems. In order to model and simulate the frictional contact between two solid bodies, both the geometric condition of non-penetration and the development of constitutive laws are required for the mechanical description of the surface interaction. The constitutive models for contact friction are based on the Coulomb friction law [6]. The constraints to be imposed at the contact surface are given in the form of inequalities and two approaches, which have received great attention in the imposition of contact constraints, are the Lagrange multiplier method and the penalty method. In the penalty method, these constraints are only approximated and the quality of the approximation depends strongly on the choice of the penalty parameter [7]. In the Lagrange multiplier method, the inequality constraints are imposed directly to the problem by the addition of contact constraints as equations to be solved simultaneously with the equilibrium equations, composing a system of non-linear equations in displacements and contact forces [8]. In the present study, XFEM and EFGM have been employed to model the frictional contact behavior between the solid bodies. Three model problems having discontinuities due to frictional contact have been analyzed and the results obtained by the two methods are compared with each other and are found quite satisfactory. In the first problem, the contact friction behavior of two sliding elastic bodies is modeled and simulated whereas in the second problem, the contact behavior of steel rod and concrete is simulated under torsional loading. The third problem models and simulates the contact behavior of a rectangular component with a circular rod at the centre under both compressive and tangential loadings.

## II. THE EXTENDED FINITE ELEMENT METHOD

The extended finite element method (XFEM) is an accurate and powerful technique to model various types of discontinuities in solid mechanics problems. This method does not consider any type of discontinuity during mesh generation, as shown in Fig. 1. Instead, the standard displacement based approximation is modified by enriching it with additional enrichment functions, which depend upon the type of discontinuity present in the domain. Different types of enrichment functions are available for modeling different types of discontinuities. Thus, the discontinuities present in the domain are modeled independent of the mesh, which reduces most of the problems associated with mesh generation such as mesh adaption and conformal meshing. XFEM has been most widely used in solving crack growth problems, bi-material problems, contact problems etc. Different types of discontinuities present in the domain are modeled by enriching the standard finite element approximation in terms of level set and signed distance functions. The method is used to model arbitrary discontinuities by enriching the discontinuous approximation in terms of signed distance and level set functions [9] through a partition of unity method [10]. Till now XFEM has been most widely applied in solving crack problems, including crack growth with frictional contact [11], cohesive crack propagation [12], fatigue crack propagation [13], crack growth under cyclic contact loading [14] and three-dimensional crack propagation [15]. XFEM has also been implemented to solve some plasticity problems including the plasticity forming of powder compaction [16], large XFEM deformations [17], crack propagation in plastic fracture mechanics [18] and quasi-brittle fracture [19].

**Manuscript published on 30 April 2014.**
***** Correspondence Author (s)
**Azher Jameel**, Department of Mechanical and Industrial Engineering, Indian Institute of Technology, Roorkee, India.

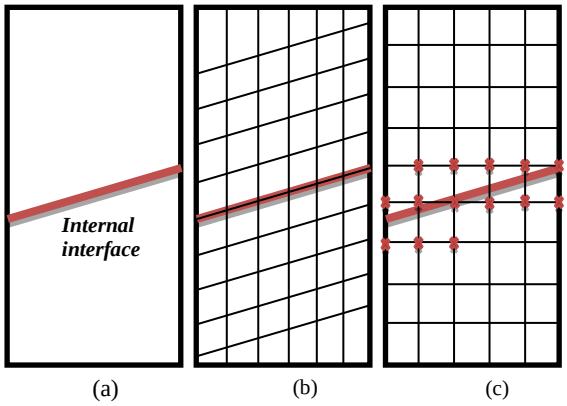


**Fig 1:** Modeling of internal interface between two bodies: (a) problem definition (b) FEM mesh which conforms to the geometry of the interface (c) XFEM mesh in which the marked nodes have additional degrees of freedom and enrichment functions

## III. THE ELEMENT FREE GALERKIN METHOD

In EFGM, the entire domain is represented by a set of nodes (Fig. 2) and the approximate function is constructed from this set of nodes over the given domain. There is no need of generating a finite element mesh in this method. EFGM was developed to eliminate the dependence of the approximate function on the finite element mesh. Thus, various problems associated with the mesh generation are eliminated by this method. EFGM enriches the standard displacement based approximation with enrichment functions in order to model different types of discontinuities present in structural problems. EFGM is very helpful in modeling large deformation problems because the finite element mesh undergoes severe distortion in these cases and remeshing is required quite frequently during the process of simulation. However, EFGM does not impose any such problem while modeling large deformation because of its meshless nature. This method proves to be very accurate and powerful for modeling different types of discontinuities in solid mechanics problems. Most applications of the EFGM technique have been reported in modeling crack growth, crack propagation, contact problems etc.

The element free Galerkin method is a meshfree method which is particularly useful for modeling arbitrary crack propagations. Meshfree methods were developed in the late 1970's. Till now meshfree methods have been used in solving various problems such as modeling astrophysical phenomena [20], tensile instability in SPH [21], coupling of smooth particle hydrodynamics with the finite element method [22] and fracture and crack growth [23].

## IV. CHOICE OF ENRICHMENT FUNCTION

The essence of XFEM and EFGM lies in the selection of an appropriate enrichment function depending upon the nature of the discontinuity present in the domain. Different types of discontinuities are modeled by different enrichment functions. The level set method is the commonly used method employed to solve discontinuous problems. The sign of the level set is positive on one side of the interface and negative on the other side of the interface. The value of the level set is always zero on the discontinuity.

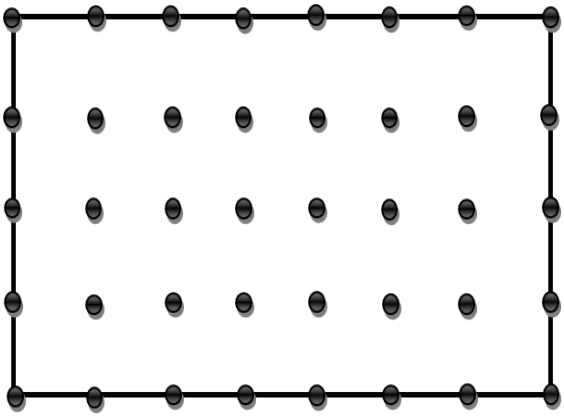

**Fig. 2:** Domain representation in EFGM

Generally, those discontinuities which arise due to variation of material properties, on the either of the discontinuity, are modeled by two types of enrichment functions. The bi-material problems have a continuous displacement field along the material interface, but the strain field is discontinuous along the discontinuity. The enrichment function employed to model bi-material problems employs the absolute value of the level set function [9]. This type of enrichment function produces a continuous displacement field and discontinuous strain field along the material interface.

The discontinuities which arise due to the contact surfaces or cracks are modeled by the Heaviside enrichment function. Let us take any point $\mathbf{x}$ in the domain, as shown in Fig. 3. Let $\mathbf{x}^*$ be the point closest to $\mathbf{x}$ on the contact interface and $\mathbf{n}$ be the unit normal to the contact surface. The Heaviside jump function $\mathrm{H}(\mathbf{x})$ is given

$$f^3(\mathbf{x}) = H(\mathbf{x}) = \begin{cases} +1 & \text{if } (\mathbf{x} - \mathbf{x}^*) \cdot \mathbf{n} \geq \mathbf{0} \\ -1 & \text{otherwise} \end{cases} \qquad (1)$$

The Heaviside jump function is a very powerful tool for modeling strong discontinuities like crack interfaces, contact surfaces etc.

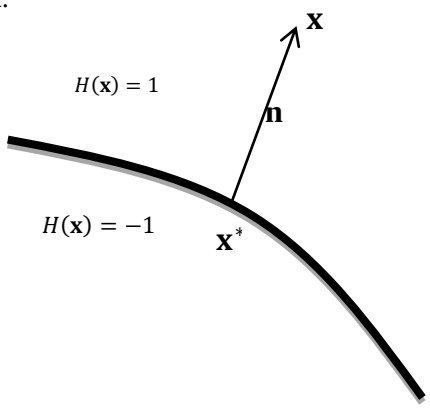


**Fig. 3: Illustration of the Heaviside jump function for a contact surface**

## V. CONSTITUTIVE MODEL FOR CONTACT FRICTION

The constitutive model for contact friction provides a theoretical description of the contact between the two bodies. Let us take a master body (M), which comes into contact with a slave body (S).


Published By:
Blue Eyes Intelligence Engineering
and Sciences Publication (BEIESP)

The basic contact problem has been shown in Fig. 4. The minimum distance (gap) between the master body and the slave body is defined as the gap ($\boldsymbol{g}_N$) between the two bodies. The contact inequalities can be written as

$$\boldsymbol{g}_N \geq 0 \quad (2a)$$
$$\mathbf{P}_N \leq 0 \quad (2b)$$
$$\mathbf{P}_N \boldsymbol{g}_N = 0. \quad (2c)$$

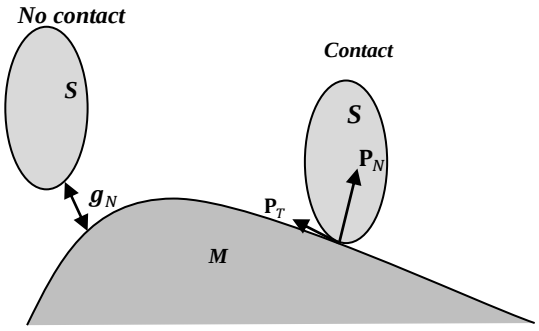


**Fig. 4:** Sliding contact between two bodies

The contact constraints may be imposed either by using the Lagrange multiplier method [25] or the penalty method [26]. The Lagrange multiplier method imposes the contact constraints directly by the addition of the contact constraints as equations to be solved simultaneously with the equilibrium equations [8]. On the contrary, the penalty method implements the springs on the contact surface in the normal and the tangential directions. The normal and the tangential forces generated in the contact zone are related to the displacements in the contact zone by means of penalty parameters. In the present study, the penalty method has been employed for the application of the contact constraints. Thus, we have

$$\mathbf{P}_N = -k_N \, \mathbf{u}_N \quad (3a)$$

$$\mathbf{P}_T = -k_T \, \mathbf{u}_T \quad (3b)$$

where, the penalty factors $k_N$ and $k_T$ may be considered as being the normal stiffness constant and shear stiffness constant, respectively.

The constitutive laws for the contact forces at the contact interface between the two bodies establish the relationship between the forces and the displacements at the contact surface. The constitutive laws for the contact loads at the contact surface can be summarized as

$$\boldsymbol{P}_N = \left(\mathbf{D}_f\right)_N \boldsymbol{u}_C \quad (4a)$$
$$\boldsymbol{P}_T = \left(\mathbf{D}_f\right)_T \boldsymbol{u}_C \quad (4b)$$

where $\left(\mathbf{D}_f\right)_N$ and $\left(\mathbf{D}_f\right)_T$ are the normal and tangential components of the friction tangent matrix and $\boldsymbol{u}_C = [\boldsymbol{u}_N \quad \boldsymbol{u}_T]^T$. The problem is artificially decomposed into a pure contact in the normal direction and frictional resistance in the tangential direction [27], which are linearized separately as $\mathrm{d}\mathbf{P} = \mathbf{D}_f \mathrm{d}\boldsymbol{u}_C$, where $\mathbf{D}_f$ is the friction tangent tensor, $\mathrm{d}\mathbf{P} = [\mathrm{d}\mathbf{P}_N \quad \mathrm{d}\mathbf{P}_T]^T$ and $\mathrm{d}\boldsymbol{u}_C = [\mathrm{d}\mathbf{u}_N \quad \mathrm{d}\mathbf{u}_T]^T$. The friction tangent matrix is defined as

$$\mathbf{D}_f = \begin{bmatrix} \mathrm{E}_f & 0 \\ 0 & \mathrm{G}_f \end{bmatrix} \quad (5)$$

The normal loads are measured by means of the linear equation $\mathbf{P}_N = E_f \mathbf{u}_N$, where $E_f$ is a normal penalty parameter. The tangential load at the contact surface is given by $\mathbf{P}_T = G_f \mathbf{u}_T$, where $G_f$ is tangential penalty parameter of the contact surface. Thus, the constitutive model for the contact friction, which relates the forces in the contact zone to the displacements in the contact zone, can be written as

$$\begin{Bmatrix} \mathrm{d}\mathbf{P}_N \\ \mathrm{d}\mathbf{P}_T \end{Bmatrix} = \begin{bmatrix} \mathrm{E}_f & 0 \\ 0 & \mathrm{G}_f \end{bmatrix} \begin{Bmatrix} \mathrm{d}\mathbf{u}_N \\ \mathrm{d}\mathbf{u}_T \end{Bmatrix} \quad (6)$$

## VI. CONTACT FRICTION MODELING WITH XFEM

The extended finite element method (XFEM) does not consider the contact surface during mesh generation. Instead, the standard approximation is modified by enriching it with the Heaviside jump function. The equilibrium equation of any deformable body can be written as

$$\int_\Omega \boldsymbol{\sigma} : \boldsymbol{\varepsilon} \, \mathrm{d}\Omega - \int_\Omega \mathbf{b} \cdot \mathbf{u} \, \mathrm{d}\Omega - \int_{\Gamma_t} \mathbf{t} \cdot \mathbf{u} \, \mathrm{d}\Gamma_t = 0 \quad (7)$$

In case of XFEM, the contact interface is taken into account by enriching the displacement field with Heaviside jump function. The displacement field is given by

$$\mathbf{u}^h(\boldsymbol{x}) = \sum_i N_i(\boldsymbol{x}) \mathrm{u}_i + \sum_j N_j(\boldsymbol{x})(H(\boldsymbol{x}) - H(\boldsymbol{x}_j)) \mathbf{a}_j \quad (8)$$

for $n_i \in \mathbf{n}$ and $n_j \in \mathbf{n}_g$

Here, $\mathrm{u}_i$ and $\mathrm{a}_j$ denote the nodal and the enriched degrees of freedom, respectively. In Eq. (8), $\mathbf{n}$ denotes the nodes of the entire domain and $\mathbf{n}_g$ denotes the nodes of the elements cut by the contact surface. $N_i$ denotes the classical finite element shape function and $H(\boldsymbol{x})$ denotes the Heaviside jump function. Eq. (8) can be further written as

$$\begin{Bmatrix} \mathrm{u} \\ \mathrm{v} \end{Bmatrix} = \begin{bmatrix} N_i & 0 \\ 0 & N_i \end{bmatrix} \begin{Bmatrix} \mathrm{u}_i \\ \mathrm{v}_i \end{Bmatrix} + \begin{bmatrix} \bar{N}_j & 0 \\ 0 & \bar{N}_j \end{bmatrix} \begin{Bmatrix} \mathrm{a}_j \\ \mathrm{b}_j \end{Bmatrix} = \mathbf{N}\mathbf{u} + \bar{\mathbf{N}}\mathbf{a} \quad (9)$$

where $\bar{N}_j = N_j(\boldsymbol{x})(H(\boldsymbol{x}) - H(\boldsymbol{x}_j))$., $\mathbf{u} = [\mathrm{u_i} \ \mathrm{v_i}]^T$ is a vector of nodal degrees of freedom, $\mathbf{a} = [\mathrm{a}_j \ \mathrm{b}_j]^T$ is a vector of enriched degrees of freedom, $\mathbf{N} = \begin{bmatrix} N_i & 0 \\ 0 & N_i \end{bmatrix}$ and $\bar{\mathbf{N}} = \begin{bmatrix} \bar{N}_j & 0 \\ 0 & \bar{N}_j \end{bmatrix}$.

The strain tensor can be written as

$$\begin{Bmatrix} \varepsilon_x \\ \varepsilon_y \\ \varepsilon_{xy} \end{Bmatrix} = \mathbf{B}\mathbf{u} + \bar{\mathbf{B}}\mathbf{a} \quad (10)$$

where

$$\mathbf{B} = \begin{bmatrix} \frac{\partial N_i}{\partial x} & 0 \\ 0 & \frac{\partial N_i}{\partial y} \\ \frac{\partial N_i}{\partial y} & \frac{\partial N_i}{\partial x} \end{bmatrix} \text{ and } \bar{\mathbf{B}} = \begin{bmatrix} \frac{\partial \bar{N}_j}{\partial x} & 0 \\ 0 & \frac{\partial \bar{N}_j}{\partial y} \\ \frac{\partial \bar{N}_j}{\partial y} & \frac{\partial \bar{N}_j}{\partial x} \end{bmatrix} \quad (11)$$

Substitution of the trial function of Eq. (8) into the equilibrium equation (7) gives the discrete system of equations as

$$\begin{bmatrix} \mathbf{K}^{uu} & \mathbf{K}^{ua} \\ \mathbf{K}^{au} & \mathbf{K}^{aa} \end{bmatrix} \begin{Bmatrix} \mathbf{u} \\ \mathbf{a} \end{Bmatrix} = \begin{Bmatrix} \mathbf{f} \\ \bar{\mathbf{f}} \end{Bmatrix} \quad (12)$$

where

$$\mathbf{K}^{\alpha\beta} = \int_{\Omega^e} (\mathbf{B}^\alpha)^T \mathbf{D}^{ep} \, \mathbf{B}^\beta \mathrm{d}\Omega \qquad (\alpha, \beta = u, a) \quad (13a)$$


Published By:
Blue Eyes Intelligence Engineering
and Sciences Publication (BEIESP)

$$\mathbf{f}^{\alpha} = \int_{\Gamma^e} \boldsymbol{N}^{\alpha}\mathbf{t}\,d\Gamma + \int_{\Omega^e} \boldsymbol{N}^{\alpha}\mathbf{b}\,d\Omega \qquad (\alpha = u, a) \qquad (13b)$$

where $\mathbf{D}^{ep}$ is the elasto-plastic constitutive matrix, $\boldsymbol{N}^{u} = \boldsymbol{N}$, $\boldsymbol{N}^{a} = \bar{\boldsymbol{N}}$, $\mathbf{B}^{u} = \mathbf{B}$, $\mathbf{B}^{a} = \bar{\mathbf{B}}$.

The contact surface is modeled by employing the Heaviside jump function as the enrichment function. While modeling frictional contact problems, it is necessary to satisfy the contact constraints at the contact interface. The modified displacement field at the contact surface is expressed as

$$\boldsymbol{u}_C(\boldsymbol{x}) = \boldsymbol{N}^{con}\mathbf{u} + \bar{\boldsymbol{N}}^{con}\mathbf{a} \qquad (14)$$

where $\boldsymbol{u}_C(\boldsymbol{x}) = [u_N \; u_T]^T$. $u_N$ represents the normal displacement and $u_T$ denotes the tangential displacement at the contact interface. The directional shape functions $\boldsymbol{N}^{con}$ and $\bar{\boldsymbol{N}}^{con}$ in normal and tangential directions can be obtained as

$$\boldsymbol{N}^{con} = \begin{bmatrix} n_1 & n_2 \\ t_1 & t_2 \end{bmatrix}\begin{bmatrix} N_i & 0 \\ 0 & N_i \end{bmatrix} \qquad (15)$$

$$\bar{\boldsymbol{N}}^{con} = \begin{bmatrix} n_1 & n_2 \\ t_1 & t_2 \end{bmatrix}\begin{bmatrix} \bar{N}_j & 0 \\ 0 & \bar{N}_j \end{bmatrix} \qquad (16)$$

For contact elements, the strains (at the contact surface) are related to the displacements (at the contact surface) by means of the matrix $\mathbf{B}^{con}$, which can be obtained as $\mathbf{B}^{con} = 2\bar{\boldsymbol{N}}^{con}_{top} = -2\bar{\boldsymbol{N}}^{con}_{bot}$. Thus, the contact stiffness matrix $\mathbf{K}^{con}$ can be obtained as

$$\mathbf{K}^{con} = \int_{\Omega^e}(\mathbf{B}^{con})^T\mathbf{D}_f\,(\mathbf{B}^{con})d\Omega \qquad (17)$$

Finally, the total stiffness matrix of an enriched element cut by the contact interface can be obtained as

$$\mathbf{K} = \begin{bmatrix} \mathbf{K}^{uu} & \mathbf{K}^{ua} \\ \mathbf{K}^{au} & \mathbf{K}^{aa} + \mathbf{K}^{con} \end{bmatrix} \qquad (18)$$

## VII. CONTACT FRICTION MODELING WITH EFGM

The modeling and simulation of frictional contact in element free galerkin method is quite easy than finite element method from computational point of view because no mesh is used to represent the domain. Therefore, the problems associated with conformal meshing, remeshing and mesh adaption do not occur in EFGM. The contact surface is taken into account by enriching the standard displacement field with Heaviside jump function. The modified displacement field can be expressed as

$$\mathbf{u}^h(\boldsymbol{x}) = \sum_i \Psi_i(\boldsymbol{x})\mathrm{u}_i + \sum_j \Psi_j(\boldsymbol{x})(H(\boldsymbol{x}) - H(\boldsymbol{x}_j))\mathrm{a}_j \qquad (19)$$

for $n_i \in \mathbf{n}$ and $n_j \in \mathbf{n}_g$

Here, $\mathrm{u}_i$ and $\mathrm{a}_j$ denote the nodal and the enriched degrees of freedom, respectively. In Eq. (19), $\mathbf{n}$ denotes the nodes of the whole domain and $\mathbf{n}_g$ denotes the nodes situated at the contact surface. $\Psi_i$ denotes the MLS shape function used in EFGM and $H(\boldsymbol{x})$ denotes the Heaviside jump function Eq. (19) can be further written as

$$\begin{Bmatrix} \mathrm{u} \\ \mathrm{v} \end{Bmatrix} = \begin{bmatrix} \Psi_i & 0 \\ 0 & \Psi_i \end{bmatrix}\begin{Bmatrix} \mathrm{u_i} \\ \mathrm{v_i} \end{Bmatrix} + \begin{bmatrix} \bar{\Psi}_j & 0 \\ 0 & \bar{\Psi}_j \end{bmatrix}\begin{Bmatrix} \mathrm{a_j} \\ \mathrm{b_j} \end{Bmatrix} = \boldsymbol{\Psi}\mathbf{u} + \bar{\boldsymbol{\Psi}}\mathbf{a} \qquad (20)$$

where $\bar{\Psi}_i = \Psi_i(H(\boldsymbol{x}) - H(\boldsymbol{x}_j))$, $\mathbf{u} = [\mathrm{u_i} \; \mathrm{v_i}]^T$ is a vector of nodal degrees of freedom, $\mathbf{a} = [\mathrm{a}_j \; \mathrm{b}_j]^T$ is a vector of enriched degrees of freedom, $\boldsymbol{\Psi} = \begin{bmatrix} \Psi_i & 0 \\ 0 & \Psi_i \end{bmatrix}$ and $\bar{\boldsymbol{\Psi}} = \begin{bmatrix} \bar{\Psi}_j & 0 \\ 0 & \bar{\Psi}_j \end{bmatrix}$.

The strain tensor can be expressed in the following form

$$\begin{Bmatrix} \varepsilon_x \\ \varepsilon_y \\ \varepsilon_{xy} \end{Bmatrix} = \mathbf{B}\mathbf{u} + \bar{\mathbf{B}}\mathbf{a} \qquad (21)$$

where

$$\mathbf{B} = \begin{bmatrix} \frac{\partial \Psi_i}{\partial x} & 0 \\ 0 & \frac{\partial \Psi_i}{\partial y} \\ \frac{\partial \Psi_i}{\partial y} & \frac{\partial \Psi_i}{\partial x} \end{bmatrix} \text{ and } \bar{\mathbf{B}} = \begin{bmatrix} \frac{\partial \bar{\Psi}_j}{\partial x} & 0 \\ 0 & \frac{\partial \bar{\Psi}_j}{\partial y} \\ \frac{\partial \bar{\Psi}_j}{\partial y} & \frac{\partial \bar{\Psi}_j}{\partial x} \end{bmatrix} \qquad (22)$$

The above matrix equation can be written in a more compact form as

$$\begin{bmatrix} \mathbf{K}^{uu} & \mathbf{K}^{ua} \\ \mathbf{K}^{au} & \mathbf{K}^{aa} \end{bmatrix}\begin{Bmatrix} \mathbf{u} \\ \mathbf{a} \end{Bmatrix} = \begin{Bmatrix} \mathbf{f} \\ \bar{\mathbf{f}} \end{Bmatrix} \qquad (23)$$

where

$$\mathbf{K}^{\alpha\beta} = \int_{\Omega^e}(\mathbf{B}^{\alpha})^T\mathbf{D}^{ep}\,\mathbf{B}^{\beta}d\Omega \qquad (\alpha, \beta = u, a) \qquad (24a)$$

$$\mathbf{f}^{\alpha} = \int_{\Gamma^e} \boldsymbol{\Psi}^{\alpha}\mathbf{t}\,d\Gamma + \int_{\Omega^e} \boldsymbol{\Psi}^{\alpha}\mathbf{b}\,d\Omega \qquad (\alpha = u, a) \qquad (24b)$$

where, $\boldsymbol{\Psi}^{u} = \boldsymbol{\Psi}$, $\boldsymbol{\Psi}^{a} = \bar{\boldsymbol{\Psi}}$, $\mathbf{B}^{u} = \mathbf{B}$, $\mathbf{B}^{a} = \bar{\mathbf{B}}$.

The contact surface is modeled by employing the Heaviside jump function as the enrichment function. While modeling frictional contact problems, it is necessary to satisfy the contact constraints at the contact interface. The modified displacement field at the contact surface is expressed as

$$\boldsymbol{u}_C(\boldsymbol{x}) = \boldsymbol{\Psi}^{con}\mathbf{u} + \bar{\boldsymbol{\Psi}}^{con}\mathbf{a} \qquad (25)$$

where $\boldsymbol{u}_C(\boldsymbol{x}) = [u_N \; u_T]^T$. $u_N$ represents the normal displacement and $u_T$ denotes the tangential displacement. Then, the directional shape functions $\boldsymbol{\Psi}^{con}$ and $\bar{\boldsymbol{\Psi}}^{con}$ in normal and tangential directions can be obtained as

$$\boldsymbol{\Psi}^{con} = \begin{bmatrix} n_1 & n_2 \\ t_1 & t_2 \end{bmatrix}\begin{bmatrix} \Psi_i & 0 \\ 0 & \Psi_i \end{bmatrix} \qquad (26)$$

$$\bar{\boldsymbol{\Psi}}^{con} = \begin{bmatrix} n_1 & n_2 \\ t_1 & t_2 \end{bmatrix}\begin{bmatrix} \Psi_j H & 0 \\ 0 & \Psi_j H \end{bmatrix} \qquad (27)$$

The strain matrix $\mathbf{B}^{con}$ relating the strain and nodal displacements at the contact interface can be obtained as $\mathbf{B}^{con} = 2\bar{\boldsymbol{\Psi}}^{con}_{top} = -2\bar{\boldsymbol{\Psi}}^{con}_{bot}$. Thus, the contact stiffness matrix $\mathbf{K}^{con}$ can be obtained as

$$\mathbf{K}^{con} = \int_{\Omega^e}(\mathbf{B}^{con})^T\mathbf{D}_f\,(\mathbf{B}^{con})d\Omega \qquad (28)$$

Finally, the total stiffness matrix of an enriched node at the contact interface can be obtained as

$$\mathbf{K} = \begin{bmatrix} \mathbf{K}^{uu} & \mathbf{K}^{ua} \\ \mathbf{K}^{au} & \mathbf{K}^{aa} + \mathbf{K}^{con} \end{bmatrix} \qquad (29)$$

## VIII. NUMERICAL RESULTS AND DISCUSSIONS

Now, we consider some numerical problems that were solved to find out the applicability and versatility of XFEM and EFGM in modeling the discontinuities that are caused by the frictional contact. The results obtained by XFEM are compared with the results obtained by EFGM and a very good agreement is observed between the two methods after the comparison of the results.


Published By:
Blue Eyes Intelligence Engineering
and Sciences Publication (BEIESP)

Three 2D problems are modeled and simulated using both the techniques. The first problem models and simulates the contact behavior between two solid bodies that are free to slide over each other. The second problem models and simulates the behavior of a steel rod in concrete under torsional loading. The last example investigates the contact behavior of a rectangular block with a circular rod placed at the centre. The results show that the two techniques can be efficiently used to solve the solid mechanics problems having discontinuities caused by the frictional contact.

### *A. Contact Friction Behavior between Two Sliding Bodies*

The first problem models and simulates the contact behavior between two elastic bodies which are free to slide over each other by both XFEM and EFGM. The block is constrained at the bottom while the top edge of the block is subjected to the uniform vertical and horizontal loadings of $w_y = 1 \times 10^5$ N/m and $w_x = 2.5 \times 10^4$ N/m, respectively. The Young's modulus has been assumed to be $2 \times 10^{11}$ N/m$^2$ for the blocks and Poisson's ratio has been taken as $0.3$. The geometry of the block is shown in Fig. 5. The length and width of the block are both unity. The state of plane stress is taken for the sake of analysis. Plane stress condition has been assumed for analysis. The normal penalty parameter of the contact surface has been taken to be $1 \times 10^{10}$ N/m$^2$ and the tangential penalty parameter has been assumed to be $1 \times 10^8$ N/m$^2$.

A uniform mesh of 361 elements has been considered in XFEM simulation, as shown in Fig. 6. The numerical simulation is also performed in EFGM using 400 nodes with a nodal density of $20 \times 20$, as shown Fig. 7. The load is applied in 20 increments. The distributions of shear stress $\sigma_{xy}$, normal stress $\sigma_{yy}$ and normal stress $\sigma_{xx}$ along the contact surface are shown in Fig. 8, Fig. 9and Fig. 10, respectively. The normal stresses $\sigma_{xx}$ along the top surface are shown in Fig. 11. A remarkable agreement is seen between the results obtained by XFEM and EFGM.

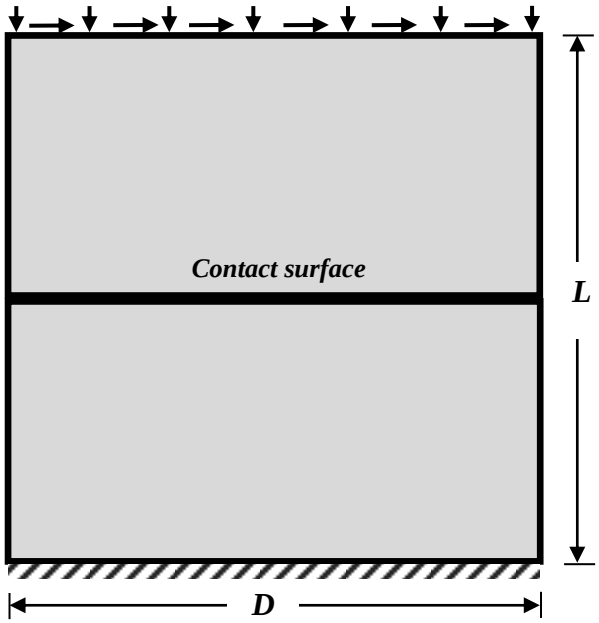


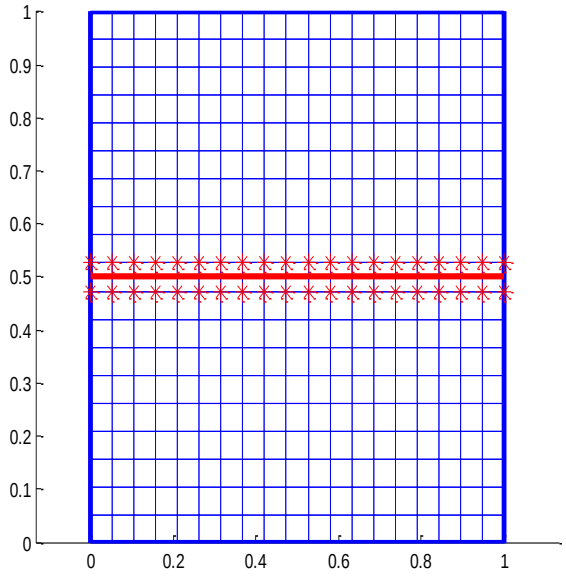

**Fig. 6:** Sliding of two bodies: XFEM mesh

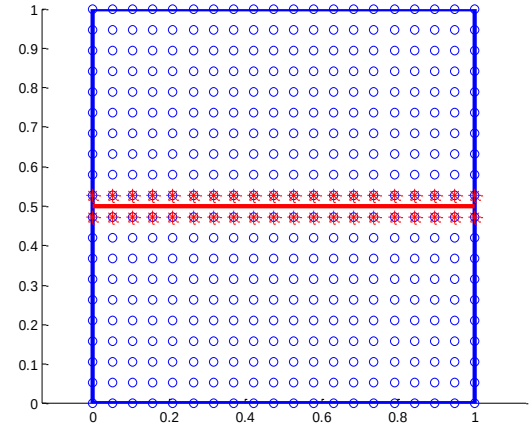

**Fig. 7:** Sliding of two bodies: EFGM domain representation

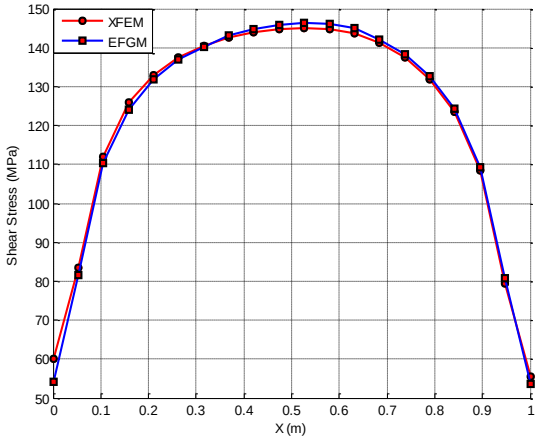


**Fig. 8:** Shear stress $\sigma_{xy}$ along the contact surface


Published By:
Blue Eyes Intelligence Engineering
and Sciences Publication (BEIESP)

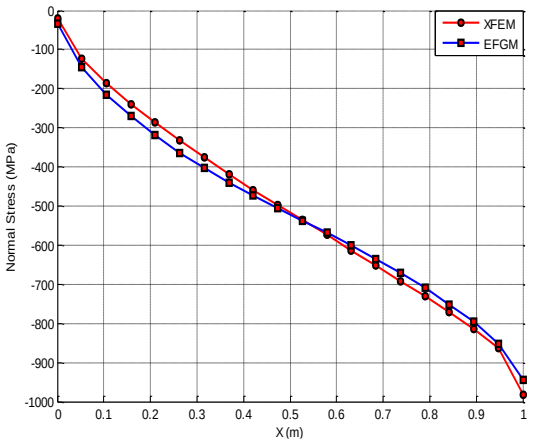


**Fig. 9:** Normal stress $\sigma_{yy}$ along the contact surface

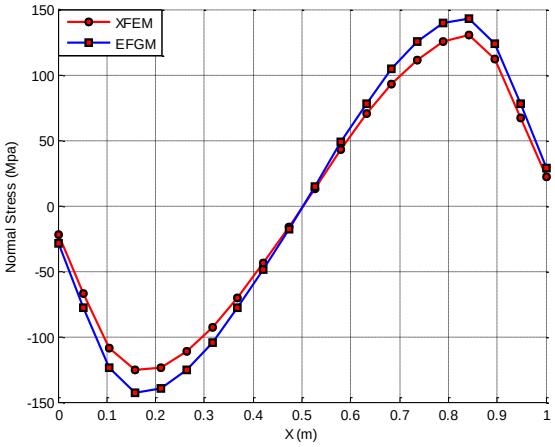


**Fig. 10:** Normal stress $\sigma_{xx}$ along the contact surface

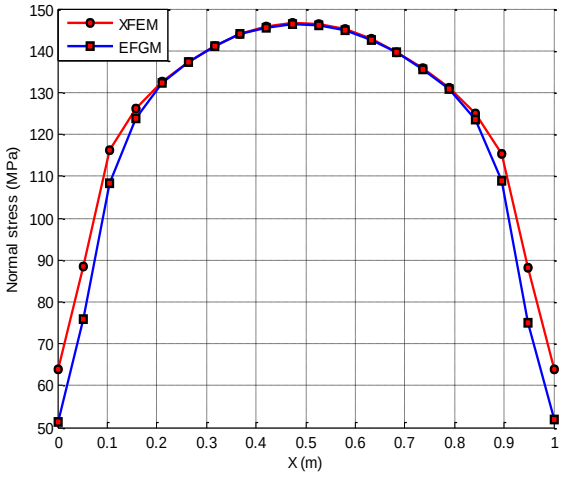


**Fig. 11:** Normal stress $\sigma_{xx}$ along the top surface

### *B. Contact Friction Behavior in Torsion of Steel Rod with Concrete*

This example models the contact behavior of a steel rod placed in concrete under torsional loading, as shown Fig. 12. The clockwise torsional moment of 0.96 ton-m is applied on the steel rod placed at the centre of a $2 \times 2$m concrete block. Plane stress condition has been considered for analysis. The material properties chosen are; $E_c = 2 \times 10^{10}$ N/ m$^2$ and $E_s = 2 \times 10^{11}$ N/ m$^2$ . The normal and tangential penalty parameters of the contact surface are chosen to be $1 \times 10^{12}$ N/ m$^2$ and $1 \times 10^{10}$ N/ m$^2$ , respectively.

In XFEM analysis, the numerical simulation is performed using a uniform mesh of 400 elements (Fig. 13), whereas in EFGM the simulation is performed using 441 nodes with a nodal density of $21 \times 21$, as shown in Fig. 14. The entire load is applied in 50 increments. The distribution of shear stress $\sigma_{xy}$ along the along the horizontal direction through the middle is shown in Fig. 15, and a good agreement is seen between the results obtained by the two methods. In Fig. 16, the normal stress $\sigma_{xx}$ is plotted along the top surface. In Fig. 17 and Fig. 18, the distribution of shear stress $\sigma_{xy}$ along the top surface and the central vertical direction are plotted. A remarkable agreement is seen between the results obtained by XFEM and EFGM in modeling and simulation of contact problems.

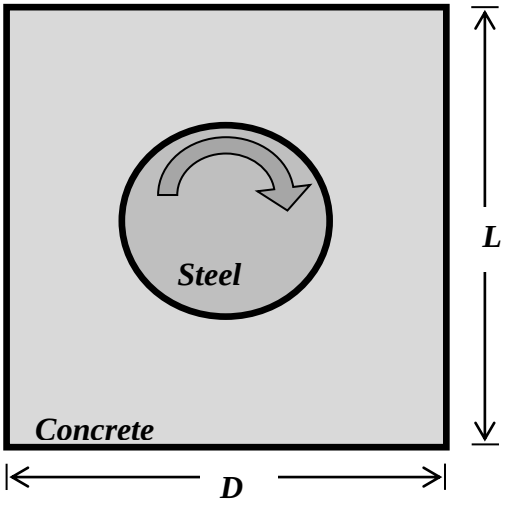


**Fig. 12:** Torsion of steel rod in concrete: Problem statement

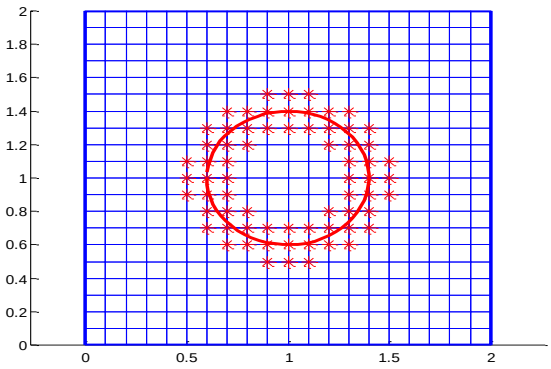

**Fig. 13:** Torsion of steel rod in concrete: XFEM mesh

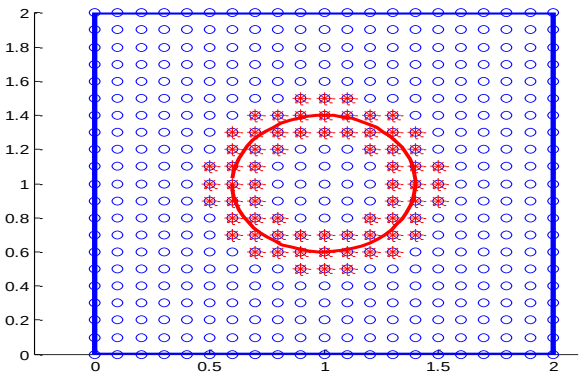

**Fig. 14:** Torsion of steel rod in concrete: EFGM domain representation


*Published By:*
*Blue Eyes Intelligence Engineering and Sciences Publication (BEIESP)*

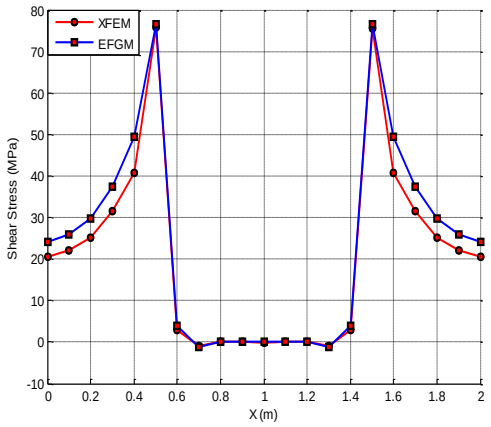


**Fig. 15:** Shear stress $\sigma_{xy}$ along the horizontal direction through the middle

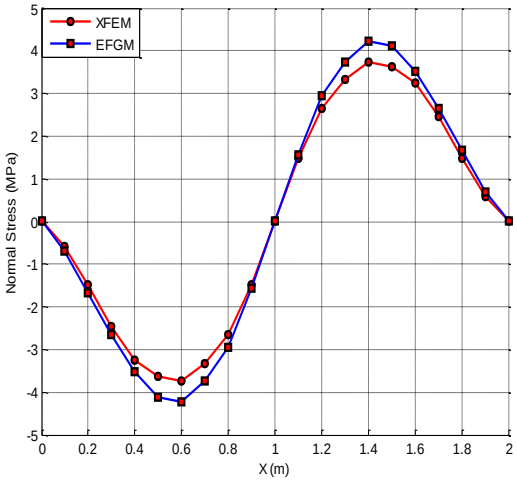


**Fig. 16:** Normal stress $\sigma_{xx}$ along the top surface

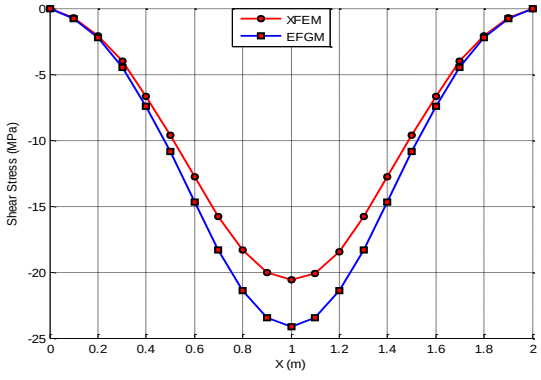


**Fig. 17:** Shear stress $\sigma_{xy}$ along the top surface

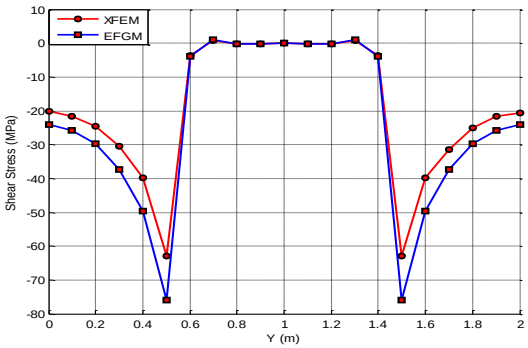


**Fig. 18:** Shear stress $\sigma_{xy}$ along the vertical direction through the middle

### *C. Contact Friction Behavior between a Circular Rod and a Rectangular Block*

This example investigates the contact behavior of a rectangular block with a circular rod at the centre, as shown in Fig. 19. The block is constrained at the bottom while the uniform horizontal and vertical loadings of $w_x = 5 \times 10^4$ N/m and $w_y = 2 \times 10^5$ N/m are imposed at the top surface. The material and the contact properties are similar to those given in the first example.

In XFEM analysis, the numerical simulation is performed using a uniform mesh of 600 elements (Fig. 20), whereas in EFGM the simulation is performed using 651 nodes with a nodal density of $21 \times 31$, as shown in Fig. 21. In Fig. 22 and Fig. 23, the shear stress $\sigma_{xy}$ and the normal stress $\sigma_{yy}$ distributions along the top surface are plotted. In all cases, a remarkable agreement is observed between the results obtained by the two methods.

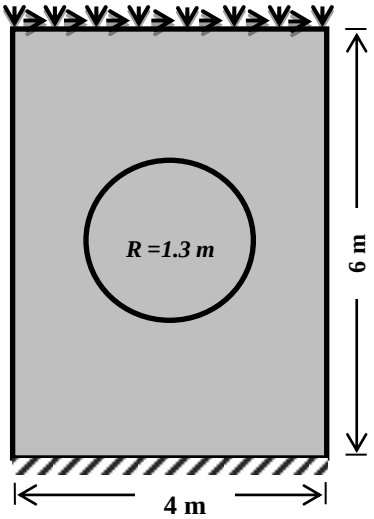


**Fig. 18:** A circular rod in a rectangular block: Problem statement

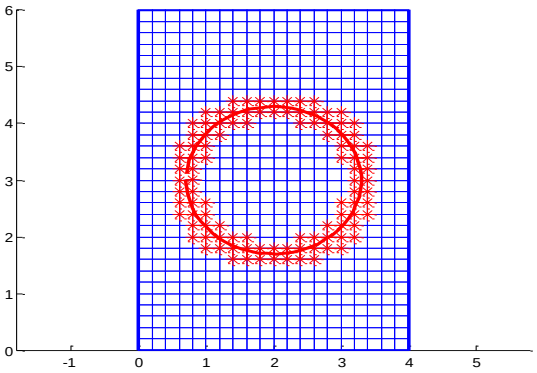

**Fig. 20:** XFEM mesh


Published By:
Blue Eyes Intelligence Engineering
and Sciences Publication (BEIESP)

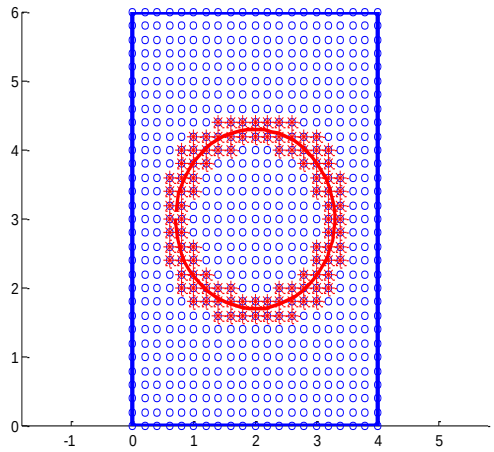

**Fig. 21:** EFGM domain representation

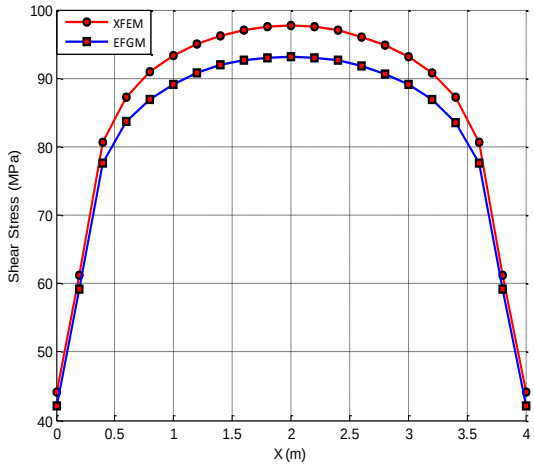


**Fig. 22:** Shear stress $\sigma_{xy}$ along the top surface

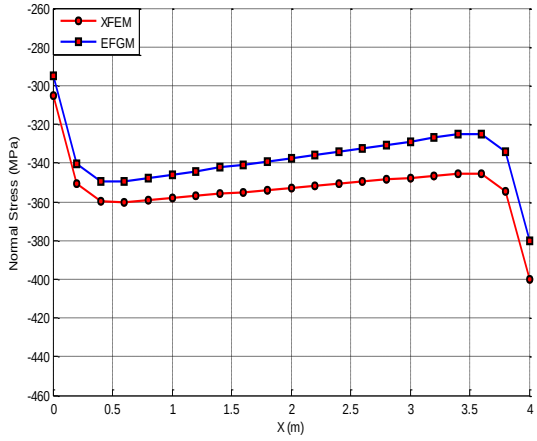


**Fig. 23:** Normal stress $\sigma_{yy}$ along the top surface

## IX. CONCLUSIONS

In this paper, extended finite element method (XFEM) and element free Galerkin method (EFGM) have been employed to model and simulate the solid mechanics problems containing discontinuities caused by the frictional contact. The classical displacement approximation was enriched with additional functions based on the Heaviside jump function to model the discontinuities caused by the contact interface. The Gauss quadrature rules for numerical integration were modified at the contact interface in order to perform numerical integration more accurately and efficiently near the contact surface.

Finally, three numerical examples are presented to demonstrate the accuracy and capability of XFEM and EFGM in the modeling and simulation of frictional contact problems. The first problem models and simulates the contact friction behavior of two sliding elastic bodies. The second problem includes the modeling of the contact behavior of the steel rod and concrete under torsional loading. The last problem models and simulates the contact behavior of a rectangular block with a circular rod at the centre. The results obtained by XFEM are compared with those obtained by EFGM and remarkable agreements were achieved between the two techniques. The results clearly indicate that the two techniques can be efficiently used to model the discontinuities caused by the frictional contact.

## REFERENCES

[1] T. Liszka, J. Orkisz, “The finite difference method at arbitrary irregular grids and its application in applied mechanics”, Computers and Structures, vol. 11, 1980, pp. 83–95.
[2] J. Oliver, A. E. Huespe, P. J. Sanchez, “A finite element method for crack growth without remeshing”, International Journal for Numerical Methods in Engineering, vol. 46, 1999, pp. 131–150.
[3] J. A. A. Portela, M. Aliabadi, D. Rooke, “The dual boundary element method: effective implementation for crack problems”, International Journal for Numerical Methods in Engineering, vol. 33, 1991, pp. 1269–1287.
[4] U. Haussler, C. Korn, “An adaptive approach with the element free Galerkin method”, Computer Methods in Applied Mechanics and Engineering, vol. 162, 1998, pp. 203–222.
[5] A. R. Khoei, S. O. R. Biabanaki, M. Anahid, “Extended finite element method for three-dimensional large plasticity deformations on arbitrary interfaces”, Computer Methods in Applied Mechanics and Engineering, vol. 197, 2008, pp. 1100–1114.
[6] J. H. Chen, N. Kikuchi, “An incremental constitutive relation of unilateral contact friction for large deformation analysis”, Journal of Applied Mechanics, vol. 52, 1985, pp. 639-648.
[7] P. Papadopoulos, R. L. Taylor, “A mixed formulation for the finite element solution of contact problems”, Computer Methods in Applied Mechanics and Engineering, vol. 94, 1992, pp. 373–389.
[8] K. J. Bathe, A. Chaudary, “A solution method for planar and axisymmetric contact problems”, International Journal for Numerical Methods in Engineering, vol. 21, 1985, pp. 65–88.
[9] N. Sukumar, D. L. Chopp, N. Moes, T. Belytschko, “Modeling holes and inclusions by level sets in the extended finite-element method”, Computer Methods in Applied Mechanics and Engineering, vol. 190, 2001, pp. 6183–6200.
[10] J. M. Melenk, I. Babuska, “The partition of unity finite element methods: basic theory and applications”, Computer Methods in Applied Mechanics and Engineering, vol. 139, 1996, pp. 289–314.
[11] J. Dolbow, N. Moes, T. Belytschko, “An extended finite element method for modeling crack growth with frictional contact”, Computer Methods in Applied Mechanics and Engineering, vol. 190, 2001, pp. 6825–6846.
[12] N. Moes, T. Belytschko, “Extended finite element method for cohesive crack growth”, Engineering Fracture Mechanics, vol. 69, 2002, pp. 813–833.
[13] I. V. Singh, B. K. Mishra, S. Bhattacharya, R. U. Patil, “The numerical simulation of fatigue crack growth using extended finite element method”, International Journal of Fatigue, vol. 36, 2012, pp. 109–119.
[14] S. Glodez, Z. Ren, “Modelling of crack growth under cyclic contact loading”, Theoretical and Applied Fracture Mechanics, vol. 30, 1998, pp. 159–173.
[15] P. M. A. Areias, T. Belytschko, “Analysis of three-dimensional crack initiation and propagation using the extended finite element method”, International Journal for Numerical Methods in Engineering, vol. 63, 2005, pp. 760–788.
[16] A. R. Khoei, A. Shamloo, A. R. Azami, “Extended finite element method in plasticity forming of powder compaction with contact friction”, International Journal of solids and structures, vol. 43, 2006, pp. 5421–5448.


*Published By:*
*Blue Eyes Intelligence Engineering and Sciences Publication (BEIESP)*

[17] M. Anahid, A. R. Khoei, "New development in extended finite element modeling of large elasto-plastic deformations", International Journal for Numerical Methods in Engineering, Vol. 75, 2008, pp. 1133–1171.
[18] B. Prabel, A. Combescure, A. Gravouil, S. Marie, "Level set X-FEM non-matching meshes: application to dynamic crack propagation in elasto-plastic media", International Journal for Numerical Methods in Engineering, vol. 69, 2006, pp. 1553–1569.
[19] S. Mariani, U. Perego, "Extended finite element method for quasi-brittle fracture", International Journal for Numerical Methods in Engineering, vol. 58, 2003, pp. 103–126.
[20] L. B. Lucy, "A numerical approach to the testing of the fission hypothesis", Astronomical Journal, vol. 82, 1977, pp. 1013-1024.
[21] J. W. Swegle, D. L. Hicks, S. W. Attaway, "Smoothed particle hydrodynamics stability analysis", Journal of Computational Physics, vol. 116, 1995, pp. 123–134.
[22] S. W. Attaway, M. W. Heinstein, J. W. Swegle, "Coupling of smooth particle hydrodynamics with the finite element method", Nuclear Engineering and Design, vol. 150, 1994, pp. 199–205.
[23] T. Belytschko, L. Gu, Y. Y. Lu, "Fracture and crack growth by element free Galerkin methods", Modeling and Simulation in Materials Science and Engineering, vol. 2, 1994, pp. 519–534.
[24] N. Moes, M. Cloirec, P. Cartraud, J. F. Remacle, "A computational approach to handle complex microstructure geometries", Computer Methods in Applied Mechanics and Engineering, vol. 192, 2003, pp. 3163–3177.
[25] J. C. Simo, T. A. Laursen, "An augmented Lagrangian treatment of contact problems involving friction", Computers and Structures, vol. 42, 1992, pp. 97–116.
[26] C. Eck, O. Steinbach, W. L. Wendland, "A symmetric boundary element method for contact problems with friction", Mathematics and Computers in Simulation, vol. 50, 1999, pp. 43–61.
[27] A. R. Khoei, M. Nikbakht, "An enriched finite element algorithm for numerical computation of contact friction problems", International Journal of Mechanical Sciences, vol. 49, 2007, pp. 183–199.

**AZHER JAMEEL,** Research Scholar Department of Mechanical and Industrial Engineering, Indian Institute of Technology Roorkee, Roorkee 247667, India,